Energetic analysis of an antigen/antibody interface: alanine scanning mutagenesis and double mutant cycles on the HyHEL-10/lysozyme interaction

Jaume Pons[1] , Arvind Rajpal[1,2] , and Jack F. Kirsch[1]

[1]Departments of Chemistry and Molecular and Cell Biology, University of California, and Center for Advanced Materials, Lawrence Berkeley National Laboratory, Berkeley, CA 94720.

[2]Present address: Molecular Sciences Dept., Pfizer Inc., Eastern Point Road, Groton, CT 06340.

*Corresponding author:

Jack F. Kirsch,

Department of Molecular and Cell Biology,

229 Stanley Hall,

University of California,

Berkeley, CA 94720.

Telephone & facsimile number: (510) 642-6368

E-mail address: jfkirsch@uclink4.berkeley.edu

Running Title: Energetic analysis of HyHEL-10/Lysozyme interaction

3&1/2" Macintosh HD disk enclosed. Manuscript is written in Microsoft Word 5.1A. Figures were generated with Kaleidagraph™ 3.0, Rasmol™ 2.6.1 and MacDraw Pro™ 1.0Ev1.

Total number of pages: 47

Number of tables: 5

Number of equations: 5

Number of schemes: 2

Number of figures: 3

Number of appendixes: 1

Abstract

Alanine scanning mutagenesis of the HyHEL-10 paratope of the HyHEL-10/HEWL complex demonstrates that the energetically important side chains (hot spots) of both partners are in contact. A plot of $\Delta\Delta G_{HyHEL\text{-}10\_mutant}$ versus $\Delta\Delta G_{HEWL\_mutant}$ for the five of six interacting side chain hydrogen bonds is linear (slope = 1). Only three of the 13 residues in the HEWL epitope contribute > 4 kcal/mol to the free energy of formation of the complex when replaced by alanine, but six of the 12 HyHEL-10 paratope amino acids do. Double mutant cycle analysis of the single crystallographically identified salt bridge, $D32_H$/K97, shows that there is a significant energetic penalty when either partner is replaced with a neutral side chain amino acid, but the $D32_HN$/K97M complex is as stable as the WT. The role of the disproportionately high number of Tyr residues in the CDR was evaluated by comparing the $\Delta\Delta G$ values of the Tyr→Phe *vs.* the corresponding Tyr→Ala mutations. The non polar contacts in the *light* chain contribute only about one half of the total $\Delta\Delta G$ observed for the Tyr→Ala mutation, while they are significantly more important in the *heavy* chain. Replacement of the $N31_L$/K96 hydrogen bond with a salt bridge, $N31D_L$/K96, destabilizes the complex by 1.4 kcal/mol. The free energy of interaction, $\Delta\Delta G_{int}$, obtained from double mutant cycle analysis showed that $\Delta\Delta G_{int}$ for any complex for which the HEWL residue probed is a major immunodeterminant is very close to the loss of free energy observed for the HyHEL-10 single mutant. Error propagation analysis of double mutant cycles shows that data of atypically high precision are required in order to use this method meaningfully, except where large $\Delta\Delta G$ values are analyzed.

Key Words: antigen, antibody, alanine scan mutagenesis, hen egg-white lysozyme, monoclonal antibody HyHEL-10, epitope mapping, double mutant cycles, protein-protein interaction.

Abbreviations:

HEWL, Hen (Chicken) egg-white lysozyme; HyHEL-10, monoclonal antibody raised against HEWL. CDR, complementary determining region; Fab-10, antigen binding fragment of HyHEL-10 antibody; scFv-10, single chain variable fragment of HyHEL-10 antibody; subscripts L and H, antibody light and heavy chain, respectively; $\Delta\Delta G_D$, change in free energy (WT-mutant); WT, wild type; K_D, dissociation constant for the scFv-10/HEWL complex; k_{on} and k_{off}, association and dissociation rate constants for the scFv-10/HEWL complex.

Crystallographically defined two-protein complexes are especially useful as starting points to evaluate the quantitative details of protein/protein interaction. Several specific additional advantages are provided by antibody/protein antigen complexes because the vast antibody recognition repertoire is isolated to the small CDR region while the remainder of the antibody is largely invariant. The interfaces of antibody/ protein antigen complexes are characterized by 650-1000 Å2 of buried surface area, 12-20 contact residues from each partner, 8-13 hydrogen bonds and an occasional salt bridge (Janin & Chothia, 1990.) These complexes also show an intermediate degree of shape complementarity at the interface (that is less than that of protease-protease inhibitor complexes, but greater than that of a T cell receptor with a major histocompatibility complex complex, (Ysern *et al.*, 1998)). The complex formed from hen egg-white lysozyme (HEWL) and the monoclonal antibody HyHEL-10 has been extensively studied in this (Kam-Morgan *et al.*, 1993; Rajpal *et al.*, 1998; Taylor *et al.*, 1998) and other laboratories (i.e. Padlan *et al.*, 1989, Smith-Gill *et al.*, 1984, Xavier & Willson, 1998).

Fourteen hydrogen bonds, 111 van der Waals contacts and one salt bridge have been crystallographically identified in the interface of the complex Fab-10/HEWL (Padlan et al., 1989). Kam-Morgan et al. (1993) showed that replacement of Arg21 with any of 8 other amino acids destabilizes the complex by ~2.2 kcal/mol. The value of $\Delta\Delta G$ effected by mutagenesis of Asp101 is however dependent on the side chain volume of the replacement amino acid. For example the D101G and D101F complexes have $\Delta\Delta G$ values of 0.2 and 2.2 kcal/mol respectively compared to WT.

Rajpal et al. (1998) found that the major HEWL immunodeterminants as defined by alanine scanning mutagenesis are Tyr20, Lys96 and Lys97 with $\Delta\Delta G$ values of 4.3, 6.5 and 5.6 kcal/mol respectively. Combinations of alanine

mutations in the HEWL epitope showed that the minor immunodeterminants buttress the major ones, thereby stabilizing the reactive conformation of the antigen (Rajpal & Kirsch, submitted for publication). The kinetics of interaction of HyHEL-10 with WT and mutant HEWL proved important in developing an experimental strategy for delineating protein docking trajectories (Taylor et al., 1998).

Previous studies on the contribution of the HyHEL-10 paratope residues have focused on the mutational analysis of the single salt bridge (Tsumoto *et al.*, 1996) and the heavy chain Tyr residues (Tsumoto *et al.*, 1995) (See Results and Discussion.). Xavier & Willson (1998) recently compared the kinetics of HEWL association with HyHEL-10 with those of the non overlapping monoclonal antibody HyHEL-5.

Although the HEWL epitope has been extensively probed, the general energetic topology of the HyHEL-10 paratope needs further analysis. The free energy changes in complex formation resulting from paratope mutation that are complementary to those already available from the epitope would allow double mutant cycle analysis (Schreiber & Fersht, 1995).

We report here the thermodynamic and kinetic results of alanine scanning mutagenesis of the HyHEL-10 paratope. Tyrosine residues were additionally replaced with Phe in order to dissect the effect of the hydroxyl group from that of the aromatic ring. Single and double mutant cycle analysis allows the evaluation of the energetic contributions of all of the putative hydrogen bond and salt bridge interactions. A salt bridge was introduced to replace the $N31_L$/K96 hydrogen bond interaction in order to test a theoretical prediction that this combination would increase the stability of the complex by 5.6 kcal/mol (Pomès *et al.*, 1995).

Results and Discussion

Mutant selection rationale

The complete data set of all determined rate and equilibrium constants, their associated standard errors and calculated $\Delta\Delta G$ values is provided in the Appendix.

Eighteen of the CDR residues of HyHEL-10 interact with HEWL (Table 1). The complexes containing alanine mutants of those amino acids whose side chains interact with HEWL, indicated by underscoring in Table 1, were investigated in order to explore individual contributions to overall stability. The tyrosines were also converted to phenylalanine to isolate the effects of the phenolic hydroxyl groups from the ring interactions. Additionally, the mutations $D32_HN$, $N31_L$ (D,E) and $W95_HF$ were introduced to evaluate the $D32_H$/K97 salt bridge, the $N31_L$/K96 hydrogen bond, and the effect of a more conservative substitution for tryptophan respectively.

The paratope residues $G30_L$ and $N92_L$ were not mutated because these amino acids make only main chain contacts in the complex. A single framework residue, $T30_H$, makes contact with HEWL; however the $T30_HA$ mutation does not affect the stability of the complex (data not shown).

Alanine mutants: paratope topology

The changes in $\Delta\Delta G$ values for the stabilities of the HyHEL-10/HEWL complexes effected by alanine and phenylalanine substitutions in the paratope are shown in Fig. 1 (top right), together with the corresponding effects for alanine

replacements in the epitope (Fig. 1, bottom right). The color coding is defined in the legend.

As a rule, the antibody hot, warm and null spot residues interact with the correspondingly important HEWL amino acids. $D32_H$ and $Y50_H$ are respective warm and hot spot exceptions that are discussed below. Previous investigations of protein/protein interaction report similar correspondence of the importance of complementary residues (Clackson & Wells, 1995; Goldman *et al.*, 1997). Such complementarity should be expected; i.e. if residue X makes a strong interaction only with Y as signaled by the large $\Delta\Delta G$ associated with an $X \rightarrow Ala$ substitution, then that specific relationship would be sharply reduced or eliminated by alteration of *either* partner. The lack of such correspondence is in fact an indication of additional interaction affecting at least one of the partners (See below.).

It is notable that six of the 12 HyHEL-10 residues in the paratope qualify as hot spots as defined in Figure 1, but only three of the 13 epitope residues fall into this category. The six HyHEL-10 hot spot side chains all contact the three dominant lysozyme hot spots. This difference in number of important affinity residues shows that stabilization of the complex is achieved by the accumulation of many productive cooperative interactions of the CDR residues with the fewer HEWL hot spots. Differences in the number of important residues between the two interfaces of a reacting pair of proteins has recently been reported for the interaction between human growth hormone and its receptor (Clackson *et al.*, 1998). These authors suggest that quantitatively important side chains placed in loops will show more cooperativity than will those located in rigid structures, such as α-helices. The HyHEL-10/HEWL interaction can be described similarly as two of the three hot spots contributed by HEWL are in an α-helix (Rajpal et al., 1998), while those from the antibody are distributed in the CDR loops.

The topology of the interaction shows that the hot spots are centrally located, but there is no clustering of hydrophobic hot spots in the core surrounded by hydrophilic residues in the periphery. Two of the three hot spots in the epitope have charged side chains, and three of the ten important residues in the paratope are hydrophilic, one is hydrophobic and six are tyrosines. Goldman et al. (1997) have noted that there appear to be two topological classes of protein/protein interaction. The first consists of a hydrophobic core surrounded by hydrophilic amino acids, and is exemplified by protein hormone/receptor complexes (Wells, 1996). The second is found in reactions of antibodies with protein antigens where hydrophobic and hydrophilic residues are not clustered (Dall'Acqua *et al.*, 1996, this work).

Role of salt bridges

The ε-amino group of HEWL K97 forms a salt bridge with the side chain carboxylate of $D32_H$ in the crystallographic structure of HEWL with Fab-10 (Padlan et al., 1989). These authors also noted a highly polar H-bond between the ε-amino group of HEWL K96 and Oδ1 of $N31_L$. Computational studies by Pomès et al. (1995) suggested that this H-bond might be converted to a salt bridge by placing a negatively charged residue at position $N31_L$, resulting in a calculated 5.6 kcal/mol increase in the stability of the complex.

To study the contributions of the above described interactions to the stability of this complex, the previously prepared HEWL mutants K97A, K97M and K96A (Taylor et al., 1998) were employed together with the HyHEL-10 mutants $D32_HA$, $D32_HN$, $N31_LA$, $N31_LD$ and $N31_LE$. A double mutant cycle approach was applied to each interaction.

The double mutant cycle describing the effect of Ala replacements of HEWL K97 and of HyHEL-10 $D32_H$ on the thermodynamics of complex formation (Scheme 1, bottom) shows that there is a 1.3 kcal/mol *gain* in the stability of the complex when the second mutation is added to the deleterious HyHEL-10(WT)/HEWL (K97A) single mutant complex. Thus these results indicate that the role of the negative charge of the HyHEL-10 $D32_H$ is only to neutralize the uncompensated positive charge of HEWL K97. This conclusion is supported by the observation that the value for the $D32_HA$/K97M complex is also 1.1 kcal/mol less stable than that of the WT (Appendix). Thus burying the negative charge of $D32_H$ by neutralization of the Lys 97 (HEWL) is inconsequential. Further support for this hypothesis was obtained by constructing a pair of mutants designed to maintain approximately the same steric bulk of the original ion pair, but which contribute only van der Waals interactions. The stability of the $D32_HN$/K97M complex is experimentally indistinguishable from that of the WT (Scheme 1, top). Thus the salt bridge *per se* is thermodynamically insignificant.

The effects of the $D32_HA$, $D32_HN$, and $D32_HE$ mutations on the free energy of the corresponding WT HEWL complexes were evaluated calorimetrically by Tsumoto et al. (1996). The values of the $\Delta\Delta G$ of destabilization with respect to the WT complexes are close to those reported here. These mutations yield decreases in entropy of complex formation that are partially compensated by enthalpy decreases. The $D32_HN$ mutant showed the highest decrease in enthalpy, probably due to formation of a H-bond, but this mutation has a negligible effect on the stability of the complex. The decreased entropy of complex formation was interpreted in terms of an effect of a larger structural change when binding the mutant antibodies. Tsumoto *et al*, proposed that the salt bridge suppresses excess local conformational change upon association. The present work shows that the

same result in terms of free energy is obtained by mutations that anchor the protein exclusively through interactions of uncharged residues.

The role of the HEWL K96/HyHEL-10 $N31_L$ hydrogen bond was evaluated by the double mutant cycle of Scheme 2 bottom. In double mutant cycles, the changes in free energy in the double mutant complex for a pair of residues ($\Delta\Delta G_{AB\rightarrow A'B'}$) is subtracted from the sum of the two single mutations to calculate the coupling energy ($\Delta\Delta G_{int}$) between those amino acids (Equation 1):

$$\Delta\Delta G_{int} = \Delta\Delta G_{A\rightarrow A'} + \Delta\Delta G_{B\rightarrow B'} - \Delta\Delta G_{AB\rightarrow A'B'} \quad (1)$$

K96 and $N31_L$ interact only through this hydrogen bond; therefore evaluation of the $\Delta\Delta G_{int}$ in this case allows the calculation of the contribution of this hydrogen bond to the free energy of formation of the complex as 4.7 kcal/mol (Table 2). This value is close to that obtained for the single $N31_LA$ mutation in HyHEL-10 (5.2 kcal/mol); therefore the contribution of this H-bond is isolated and it is worth ~ 5 kcal/mol.

The proposal of Pomès et al. (1995) that replacement of $N31_L$ with aspartic acid to create a salt bridge and thus stabilize the complex by a calculated 5.6 kcal/mol, was tested here via the $N31_LD$ and $N31_LE$ constructs. The calculated result was not verified experimentally; rather these mutant complexes are 1.4 kcal/mol ($N31_LD$) and 5.7 kcal/mol ($N31_LE$) less stable than those formed with WT HyHEL-10 (Scheme 2 top).

The two examples discussed above demonstrate that a charged residue in the epitope can be stabilized equally or better by a neutral H-bond donor/acceptor than by a counter ion. Hendsch & Tidor (1994) have pointed out that, in the majority of cases, the expected stabilization of salt bridges is compromised by large unfavorable desolvation contributions, and Mian *et al.* (1991) have argued

that oriented dipoles are usually preferred over counter charges in stabilizing buried ionized groups. The burying of an uncompensated charge is highly unfavorable. This fact may be generally useful in dictating the specificity of antigen/antibody interactions, because antibodies that fail to compensate for charged residues will not bind well to the antigenic protein even with otherwise excellent surface complementarity. A particularly poignant demonstration of the role of salt bridges in specificity is found in the interaction between human growth hormone and its receptor, where the removal of a salt bridge by mutation of the receptor Arg43 to Leu destabilizes the complex by only 0.5 kcal/mol (Clackson et al., 1998) but this mutant receptor cross-reacts with bovine growth hormone, whereas the WT receptor does not (Goodman *et al.*, 1996; Souza *et al.*, 1995).

Role of Hydrogen bonds

The energetic contributions to the free energy of formation of the complex of 13 of the 14 H-bonds proposed from the crystallographic structure, are shown in Table 3. It is not possible to probe the main chain/main chain H-bond between $N92_L$ and HEWL R21 by site directed mutagenesis. The role of the important H-bond K96/$N31_L$ was discussed above.

The values of $\Delta\Delta G$ obtained by amino acid replacements on HyHEL-10 correspond well with those obtained by mutation of the directly interacting residues on HEWL (Fig. 2). The strong correlation between $\Delta\Delta G$ occasioned by mutation of either partner argues that single mutations (Y to F, and others to Ala) do not generally overestimate hydrogen bond contributions. Most of the significant H-bonds in the interface contribute between 1-2 kcal/mol to the free energy of stabilization, as expected (Fersht *et al.*, 1985; Alber *et al.*, 1987;

Serrano *et al.*, 1992; Goldman et al., 1997). The proposed HyHEL-10 $S31_H$/HEWL R73, $Y58_H$/G102, S91/Y20 and T30/R73 H-bonds do not contribute significantly.

One neutral-neutral H-bond stands out for its high contribution to the stability of the complex: the HyHEL-10 $N32_L$ Nδ2 with G16 O (5.1 kcal/mol, r=3.24 Å). The Nδ2 atom of $N32_L$ also appears to contact Cε1 and Cδ1 of Y20, and Cε of K96, in the crystallographic structure. Tyr20 and K96 are HEWL hot spots, and the later contacts are thus eliminated in the mutant $N32_LA$. This observation suggests that the value of 5.1 kcal/mol is an overestimate of the contribution of this H-bond. We tried to determine the energetic value for the interaction between $N32_L$ and Y20 by double mutant cycles, but no association with HEWL was observed in the double mutant, $N32_LA$/Y20A at [scFv]= 4 μM; therefore the K_D is > 8 μM. This H-bond can not be examined by double mutant cycles as the backbone oxygen of G16 can not be eliminated by site directed mutagenesis. A possible explanation for this result would be that the $N32_LA$ mutation elicits a conformational change in the antibody. This is, however, unlikely because the residue in position 32 is not a conformational determinant for the 2/11A class of CDR-L1 (Chothia *et al.*, 1989 , Martin & Thornton, 1996.), to which the corresponding CDR of HyHEL-10 belongs.

Quantitative dissection of the free energy contribution of each of the paratope tyrosine residues

Davies & Cohen (1996) and Kabat *et al.* (1977), have noted the disproportionate number of tyrosine residues in CDRs, and Mian et al. (1991) have pointed out that there is a higher percentage in the heavy chain. It has been proposed that the explanation for the overabundance of tyrosine in CDRs is that the hydroxyphenyl

side chain allows participation in both polar and apolar interactions. This is quantitatively significant for HyHEL-10, as six of the ten important paratope residues are tyrosines ($\Delta\Delta G$ Tyr $\rightarrow$ Ala > 2.7 kcal/mol). Factoring the van der Waals interactions from the H-bonding contributions was accomplished by comparing the $\Delta\Delta G$ value of the Tyr$\rightarrow$Phe *vs* the corresponding Tyr$\rightarrow$Ala mutation. The former isolates the H-bond value as nearly as can be done by site-directed mutagenesis, while the latter measures the sum of hydroxyl and ring contributions. The results given in Fig. 1 show that the $\Delta\Delta G$ associated with each Tyr$\rightarrow$Ala is invariably greater than that of the corresponding Tyr$\rightarrow$Phe mutation. The relative contributions vary however. It is notable that the nonpolar contacts in the *light* chain contribute only about one half of the total $\Delta\Delta G$ observed for the Tyr$\rightarrow$Ala mutation, while they are significantly more important in the *heavy* chain. This difference is highlighted by the plot of Fig. 3, where separate linear correlations are observed for plots of $\Delta\Delta G$(Tyr$\rightarrow$Phe) *vs* $\Delta\Delta G$(Tyr$\rightarrow$Ala) for the light and heavy chains. Any conclusion drawn from the relation of Fig. 3 must be tempered by the limitation that there are only two tyrosines in the light chain. Nonetheless the difference for each of the two light chain tyrosines is clearly outside the range of the much better defined heavy chain correlation.

The slope for the light chain tyrosine mutations is 0.5 while that for the heavy chain residues is 0.2, emphasizing the relative dominance of nonpolar interactions in the heavy chain. Consistent with this set of observations is the fact that nonpolar residues dominate the important ($\Delta\Delta G_{(X\rightarrow Ala)}$>1 kcal/mol) heavy chain contributions to the HyHEL-10 paratope (Fig. 1; 4 Tyr, 1 Trp and 1 Asp) while the converse obtains for the light chain (2 Tyr, 2 Asn). Thus, at least for the HyHEL-10/HEWL interaction, it can be concluded that the molecular

"cement" is composed of rather clearly divided nonpolar heavy chain and polar light chain contributions.

Interestingly the magnitudes of energetic contributions of the dominant tyrosines of the light chain ($Y50_L$) and heavy chain($Y50_H$) can not be rationalized readily from the structure of the complex. The large effect of the $Y50_LF$ mutation (2.4 kcal/mol) leads to the expectation of the most significant H-bond; however the closest atoms to this hydroxyl group are Cβ and Cδ of HEWL K96, at 3.57 and 3.72 Å respectively, and the closest heteroatom, the main chain O of HEWL N93, is too distant to make a H-bond (4.03 Å). Thus the explanation for the importance of this Tyr hydroxyl group is not apparent. $Y50_H$ shows the highest contribution for a paratope residue ($\Delta\Delta G$ Tyr $\rightarrow$Ala 7.4 kcal/mol), and it is the only antibody hot spot that is not in direct contact with an epitope hot spot. However, it does contact with the HEWL warm spot, R21. $Y50_H$ also makes multiple contacts with the important paratope side chains ($W95_H$, $Y96_L$, $Y58_H$), suggesting that the large contribution identified by the $Y50_HA$ mutation is the result of a structural perturbation of the paratope binding site. Rajpal & Kirsch (submitted for publication) noted that warm spot mutations affect the value of adjacent hot spots in the HEWL epitope, and suggested that the warm spot residues function as buttresses of the hot spot contributors. The preceding discussion excludes the possible role of intervening water molecules in H-bond complexes, as their positions are not apparent in a 3 Å structure.

The role of the heavy chain tyrosines was previously studied by Tsumoto et al. (1995) who converted $Y33_H$, $Y50_H$, $Y53_H$ and $Y58_H$ to Ala, Leu and Trp. The enthalpic and entropic contributions for those mutants that could be obtained in sufficient quantity were evaluated calorimetrically. The $Y33_HA$ and $Y50_HA$ constructs could not be purified by HEWL affinity chromatography, and it was

proposed that $Y33_H$ and $Y50_H$ are major contributors to the free energy of complex formation. This suggestion is supported by the present results.

The Tyr→Phe and Tyr→Ala mutations taken singly and together define the quantitative importance of the CDR tyrosines of HyHEL-10 in the formation of the HyHEL-10/HEWL complex. Padlan (1990) discussed the advantages of aromatic over aliphatic side chain amino acids in the CDRs. He pointed out that the fusion of many atoms in a ring system, immobilizes that side chain in the free antibody, while aliphatic side chains generally have more conformational entropy in the free antibody, which would have to be frozen out in the complex.

Double mutant cycles

Carter *et al.* (1984) , introduced double mutant cycle analysis to study structural changes in the active site of a tyrosyl-tRNA synthetase. Subsequent applications include those of Serrano *et al.* (1990, 1992) in barnase and Pons *et al.* (1995) in a ß-glucanase. These investigations are applications of double mutant cycles on two amino acids within the same molecule, but the technique has been recently extended to the investigation of protein/protein interactions (barnase/barstar, Frisch *et al.*, 1997; Schreiber & Fersht, 1995; Schreiber *et al.*, 1997 and D1.3/E5.2, Goldman et al., 1997 and D1.3/HEWL, Dall'Acqua *et al.*, 1998). As described above (see *Salt Bridges*), double mutant cycles allow the calculation of the free energy of interaction ($\Delta\Delta G_{int}$) between specific amino acids. A $\Delta\Delta G_{int} = 0$ is expected for completely independent mutations. The interpretation of $\Delta\Delta G_{int} \neq 0$ is model dependent, *i.e* this quantity may reflect a change in solvation resulting from the mutation of one partner in an ion pair (Horovitz *et al.*, 1990), and/or an associated conformational change (Serrano et al., 1990).

Double mutant cycles for 12 amino acid pairs in the HyHEL-10/HEWL interface were constructed to understand more fully the energetic contributions obtained for the single mutants. Seven of these 12 pairs have side chains that are appropriately positioned to form H-bonds, salt bridges or significant van der Waals contacts while the other five are well separated. The results for contacting pairs are shown in Table 2. The $\Delta\Delta G_{int}$ for any complex for which the HEWL residue probed is a major immunodeterminant, i.e. K96 or K97 (Rajpal et al., 1998), is very close to the loss of free energy observed for the HyHEL-10 single mutant *i.e.* from Equation 1.

$$\Delta\Delta G_{int} = \Delta\Delta G_{A\rightarrow A'} \qquad (2)$$

$$\therefore \quad \Delta\Delta G_{B\rightarrow B'} = \Delta\Delta G_{AB\rightarrow A'B'}$$

where A and B refer to the antibody and HEWL respectively. In other words the $\Delta\Delta G$ associated with the double mutation is realized entirely by mutation of the lysozyme hot spot.

Although the $\Delta\Delta G_{int}$ values for remote pairs of amino acids are generally small (Table 4), there are two exceptions: the $Y50_LA$/K97A and the $W95_HA$/K96A pairs. One interpretation is that the $Y50_LA$ or $W95_HA$ mutations effect a conformational change that allows the recapture elsewhere in the complex of some of the free energy lost when the K97A or K96A mutation is introduced into the WT antibody complex, e.g. $7.3 < (6.2 + 4.6)$ kcal/mol, for $Y50_LA$/K97A, because less free energy of association is lost in the double mutant than in the sum of the two single mutants). This interpretation is supported by the observation that the correspondingly more conservative $Y50_LF$ and $W95_HF$ mutants do not bind as well ($\Delta\Delta G > 8.5$ kcal/mol) to the K97A and K96A HEWL as do the $Y50_LA$ and $W95_HA$ antibodies, while the opposite situation is

obtained for association with WT HEWL (Table 4). The values of $\Delta\Delta G_{int}$ are small for the double mutant cycles not involving K96 or K97 (Table 4).

Mariuzza's laboratory has recently published the results of double mutant cycle analyses with the antibody D1.3/HEWL complexes (Dall'Acqua et al., 1998) and the D1.3/E5.2 (Goldman et al., 1997) complexes, E5.2 is an anti-idiotypic antibody. The values of K_D are both in the 10 nM range. These complexes are about 300-fold less stable than the HyHEL-10/HEWL complex. Comparison of the results of single and double mutations between high affinity and weaker complexes is instructive. A clear difference is the observation that no single amino acid in HEWL makes a comparable contribution to the free energy of association with the D1.3 antibody as do the three previously identified dominant residues of HEWL in the HyHEL-10 complex. Alanine scanning has provided values of $\Delta\Delta G$= 4.2, 7.0 and 6.1 for the Y20A, K96A and K97A complexes respectively (Rajpal et al, 1998); whereas the largest effect of an Ala replacement of HEWL in the D1.3 complex, Q121A, decreases the stability only by 2.0 kcal/mol. The same two complexes also show striking differences in alanine scanning mutagenesis of the paratope. Six of the twelve alanine substitutions in the HyHEL-10 paratope yield $\Delta\Delta G$ values $\geq$4 kcal/mol (Fig. 1), while only one of nine in the weaker D1.3/HyHEL-10 complex is that large. It may be possible that weak protein/protein association complexes contain fewer and "colder" hot spots than do the analogous tight complexes.

Errors in double mutant cycle analysis

The following considerations argue that the quantitative value of double mutant cycle results is limited to analysis of large values of $\Delta\Delta G_{int}$ unless data of

more than typical precision are collected. The propagated error in $\Delta\Delta G_{int}$ (Equation 1), $\sigma_{\Delta\Delta Gint}$ is

$$\sigma_{\Delta\Delta Gint}=\sqrt{(\sigma_{\Delta\Delta G_{A\rightarrow A'}})^2+(\sigma_{\Delta\Delta G_{B\rightarrow B'}})^2+(\sigma_{\Delta\Delta G_{AB\rightarrow A'B'}})^2} \qquad (3)$$

Typical reported errors in the determination of values of K_D range from 12 % (Frisch et al., 1997; Schreiber & Fersht, 1995; Schreiber et al., 1997) to 30% (Dall'Acqua et al., 1996; Dall'Acqua et al., 1998; Goldman et al., 1997) or a spread between those values (Ackermann *et al.*, 1998). Those reported here are 10-15%, except for very deleterious double mutants where they increase to 50% (Appendix). These values represent the reported precision not the accuracy. Some subsequent determinations of the identical constructs from the same laboratory using the same or an alternative technique yield significantly more variation.

Table 5 reports the calculated propagated errors in $\Delta\Delta G_{int}$ for a range of *per cent* errors in the individual K_D determinations. For example a 30 % error in K_D values propagates to an error of 1 kcal/mol in $\Delta\Delta G_{int}$. Many workers consider a spread of 2σ values (90% confidence level) to be a satisfactory threshold level of quantitative significance (Schreiber et al., 1997). This means, for example, that errors in K_D values must be $\leq$ 20% in order to draw meaningful conclusions for $\Delta\Delta G_{int} \leq 2$ kcal/mol. This figure falls well within the range of H-bond interactions. The conclusion is that without highly precise data, double mutant cycle analysis can only be applied with confidence to the consideration of 'hot spots".

Material and Methods

The materials and procedures not described here are to be found in Rajpal & Kirsch (submitted for publication).

HyHEL-10 expression and purification

All determinations were carried out with the scFv gene for the monoclonal antibody HyHEL-10 (scFv-10), a gift of Professor Andreas Plückthun. The scFv-10 gene was cloned with *Xho I/Avr II* into the pPIC-9 secretion vector for *Pichia pastoris* (Invitrogen). Five histidine residues were added to the C-terminus to allow Ni-column purification. The recombinant plasmid was linearized by *Stu I* restriction digest for genomic integration into *P. pastoris* GS115. Transformants were selected for their capacity to grow in histidine free media. One of ten transformants showing the highest expression level was used to express the protein in BMMY media (1% yeast extract, 2% peptone, 1.34% yeast nitrogen base, 0.5% methanol, 4 x 10^{-5} % biotin, 100 mM potassium phosphate, pH 6.0). Expression cultures were incubated at 30°C for 5 days inducing with 0.5% methanol (final concentration) every 12 h. The culture was centrifuged (11,000g, 15 min.), the supernatant collected, the pH adjusted to 7.0 with KOH, and the suspension centrifuged (11,000g, 30 min.) to remove precipitated proteins. The supernatant was loaded onto Ni-NTA (nitrolotriacetic acid) superflow resin (Qiagen) equilibrated with 66 mM potassium phosphate buffer, pH 7.0, 300 mM KCl. The column was washed with 5 volumes of 66 mM potassium phosphate buffer, pH 7.0, 300 mM KCl, and the scFv-10 was eluted with a shallow linear gradient of imidazole (0-0.3 M in the same buffer). Fractions enriched (analyzed by SDS-PAGE) with scFv-10 were pooled and

dialyzed against 66 mM potassium phosphate buffer, pH 7.0. The purity of the samples was verified by SDS-PAGE. Absence of glycosidation was confirmed by mass spectrometry and no dimers were detected by HPLC gel filtration (Bio-sil-sec 250 Column, Bio-Rad). The proteins were stored at low concentration to minimize dimerization (<0.5 mg/mL, Dougan *et al.*, 1998). Mutant proteins were concentrated by Centriprep-10 prior to use when required. The concentration of scFv-10 was determined with the molar extinction coefficient (ε_{280}= 53,200 M^{-1} cm^{-1}, calculated from the amino acid sequence and verified for the WT protein by titration with HEWL). 20 to 50 mg of purified protein per liter of culture were typically obtained.

Site directed mutagenesis

The HEWL mutant genes were available from previous investigations of this laboratory (Taylor et al., 1998; Rajpal et al., 1998). The HyHEL-10 mutants were produced by PCR with the megaprimer method (Landt *et al.*, 1990, Pons *et al.*, 1997). All mutants were fully sequenced.

Determination of kinetic parameters for complex formation and dissociation

HyHEL-10 occludes the active site of HEWL. The complex has only 5 % of the catalytic activity of free HEWL; therefore the extent of HyHEL-10 association with HEWL can be determined in homogeneous solution by monitoring the rate of loss of activity of HEWL following addition of HyHEL-10 as described by Taylor et al. (1998). The values of k_{on} were determined from nonlinear regression of the data from Equation 4.

$$Abs_{obs} = Abs_{init} + v_{bl} \bullet t - \left[\frac{k_{cat} \bullet [E_T] \bullet [S]}{k_{on} \bullet K_m \bullet [Ab_T]} \bullet e^{\left(\frac{k_{on} \bullet [Ab_T] \bullet K_m \bullet t}{K_m + [S]} \right)} \right] \quad (4)$$

where Abs_{init} = initial absorbance at 450 nm, v_{bl} = the settling rate of the substrate cell wall particles in the absence of HEWL, $[E_T]$ = total concentration of HEWL, $[Ab_T]$ = total scFv-10 concentration, and [S] = initial substrate *M. luteus* cell wall concentration. Only those fits to Equation 4 yielding a correlation coefficient, R, of ≥ 0.995 were accepted.

The dissociation rate constants, k_{off}, were determined by monitoring the rate of recovery of active HEWL from a preformed HyHEL-10/HEWL complex. The nascent free antibody was sequestered with an excess of E35Q HEWL, an inactive mutant. The data were fitted to equation 5 (Rajpal et al., 1998).

$$v_{obs} = k_{cat} \bullet [E_T] \bullet (1 - e^{-k_{off} \bullet t}) + v_{init} \bullet (e^{-k_{off} \bullet t}) + v_{bl} \quad (5)$$

where v_{init} = enzymatic activity due to the complex and trace amounts of HEWL before the addition of E35Q HEWL. The kinetic assays were performed at pH 7.0 instead of pH 6.2 in order to eliminate scFv-10 precipitation (pI = 6.0, calculated from the amino acid composition). The k_{on} and k_{off} values for the formation and dissociation of the scFv-10/HEWL(WT) complex at pH 7.0 were similar to those obtained at pH 6.2 (data not shown). All data were obtained on a Uvikon 860 (Kontron Instruments, San Diego, CA.) spectrophotometer and fitted by nonlinear regression to their respective models utilizing the application Kaleidagraph (Synergy Software, Reading, PA).

When K_D values are greater than 3 nM (100 x K_D WT) the kinetics are too fast to monitor by these methods; in these cases, only the values of K_D determined

by equilibrium methods (Kam-Morgan et al., 1993) are given. All scFv-10 concentrations were < 20 μM.

Acknowledgments

We wish to thank Professor Andreas Plückthun for the generous gift of the gene for the scFv form of HyHEL-10. We are additionally grateful to Ms.Tinh Luong for help with the analysis of the X-ray structure and Dr. Douglas Burdette for initial work on scFv expression in *Pichia pastoris*. This work was supported by the Director, Office of Energy Research, Office of Basic Energy Sciences, Divisions of Material Sciences and of Energy Biosciences of the U.S. Department of Energy under Contract No. DE-AC03-76SF00098 to Lawrence Berkeley National Laboratory. Jaume Pons was supported by a postdoctoral fellowship from Ministerio de Educación y Cultura (Spain)

References

Ackermann EJ, Ang ET, Kanter JR, Tsigelny I, Taylor P. 1998. Identification of pairwise interactions in the alpha-neurotoxin-nicotinic acetylcholine receptor complex through double mutant cycles. *J Biol Chem 273* : 10958-10964.

Alber T, Dao-Pin S, Nye JA, Muchmore DC, Matthews BW. 1987. Temperature-sensitive mutations of bacteriophage T4 lysozyme occur at sites with low mobility and low solvent accesibility in the folded protein. *Biochemistry 26* : 3754-3758.

Carter PJ, Winter G, Wilkinson AJ, Fersht AR. 1984. The use of double mutants to detect structural changes in the active site of the tyrosyl-tRNA synthetase (Bacillus stearothermophilus). *Cell 38* : 835-840.

Chothia C, Lesk AM, Tramontano A, Levitt M, Smith-Gill SJ, Air G, Sheriff S, Padlan EA, Davies D, Tulip WR, Colman PM, Spinelli S, Alzari PM, Poljak RJ. 1989. Conformations of immunoglobulin hypervariable regions. *Nature 342* : 877-883.

Clackson T, Ultsch MH, Wells JA, de Vos AM. 1998. Structural and functional analysis of the 1:1 growth hormone: receptor complex reveals the molecular basis for receptor affinity. *J Mol Biol 277* : 1111-1128.

Clackson T, Wells JA. 1995. A hot spot of binding energy in a hormone-receptor interface. *Science 267* : 383-386.

Dall'Acqua W, Goldman ER, Eisenstein E, Mariuzza RA. 1996. A mutational analysis of the binding of two different proteins to the same antibody. *Biochemistry 35* : 9667-9676.

Dall'Acqua W, Goldman ER, Wenhong L, Teng C, Tsuchiya D, Li H, Ysern X, Braden BC, Li Y, Smith-Gill SJ, Mariuzza RA. 1998. A mutational analysis of

binding interactions in an antigen-antibody protein-protein complex. *Biochemistry 37* : 7981-7991.

Davies DR, Cohen GH. 1996. Interactions of protein antigens with antibodies. *Proc Natl Acad Sci USA 93* : 7-12.

Dougan DA, Malby RL, Gruen LC, Kortt AA, Hudson PJ. 1998. Effects of substitutions in the binding surface of an antibody on antigen affinity. *Protein Eng 11* : 65-74.

Fersht AR, Shi J, Knill-Jones J, Lowe DM, Wilkinson AJ, Blow DM, Brick P, Carter P, Waye MM, Winter G. 1985. Hydrogen bonding and biological specificity analysed by protein engineering. *Nature 314* : 235-238.

Frisch C, Schreiber G, Johnson CM, Fersht AR. 1997. Thermodynamics of the interaction of barnase and barstar: changes in free energy versus changes in enthalpy on mutation. *J Mol Biol 267* : 696-706.

Goldman ER, Dall'Acqua W, Braden BC, Mariuzza RA. 1997. Analysis of binding interactions in an idiotope-antiidiotope protein-protein complex by double mutant cycles. *Biochemistry 36* : 49-56.

Goodman HM, Frick GP & Souza S. 1996. Species specificity of the primate growth hormone receptor. *News Physiol Sci 11* : 157-161.

Hendsch ZS & Tidor B. 1994. Do salt bridges stabilize proteins?, a continuum electrostatic analysis. *Protein Sci* 3: 221-226.

Horovitz A, Serrano L, Avron B, Bycroft M, Fersht AR. 1990. Strength and cooperativity of contributions of surface salt bridges to protein stability. *J Mol Biol 216* : 1031-1044.

Janin J, Chothia C. 1990. The structure of protein-protein recognition sites. *J Biol Chem 265* : 16027-16030.

Kabat EA, Wu TT, Bilofsky H. 1977. Unusual distribution of amino acids in complementarity-determining (hypervariable) segments of heavy and light

chains of immunoglobulins and their possible roles in specificity of antibody combining sites. *J Biol Chem 252* : 6609-6616.

Kam-Morgan LNW, Smith-Gill SJ, Taylor MG, Zhang L, Wilson AC, Kirsch JF. 1993. High-resolution mapping of the HyHEL-10 epitope of chicken lysozyme by site-directed mutagenesis. *Proc Natl Acad Sci USA 90* : 3958-3962.

Landt O, Grunert HP, Hahn U. 1990. A general method for rapid site-directed mutagenesis using the polimerase chain reaction. *Gene 96* :125-128.

Martin ACR, Thornton JM. 1996. Structural families in loops of homologous proteins: automatic classification, modeling and application to antibodies. *J Mol Biol 263* : 800-815.

Mian S, Bradwell AR, Olson AJ. 1991. Structure, function and properties of antibody binding sites. *J Mol Biol 217* : 133-151.

Padlan EA. 1990. On the nature of antibody combining sites: unusual structural features that may confer on these Sites an enhanced capacity for binding ligands. *Proteins: Struct Funct Genet 7* : 112-124.

Padlan EA, Silverton EW, Sheriff S, Cohen GH, Smith-Gill SJ, Davies DR. 1989. Structure of an antibody-antigen complex: Crystal structure of the HyHEL-10 Fab-lysozyme complex. *Proc Natl Acad Sci USA 86* : 5938-5942.

Pomès R, Willson RC, McCammon JA. 1995. Free energy simulations of the HyHEL-10/HEL antibody-antigen complex. *Protein Eng 8* : 663-675.

Pons J, Planas A, Juncosa M, Querol E. 1997. PCR site-directed mutagenesis using *Pyrococcus sp* GB-D polymerase coupled to a rapid screening procedure. In *PCR cloning protocols* (White BA, ed.), *Vol. 67*, pp. 209-218. Humana Press.

Pons J, Planas A, Querol E. 1995. Contribution of a disulfide bridge to the stability of 1,3-1,4-ß-D-glucan 4-glucanhydrolase from *Bacillus licheniformis*. *Protein Eng 8* : 938-945.

Rajpal A, Kirsch JF. 1998. Combinatorial alanine replacements of the minor contributors in chicken egg white lysozyme (HEWL) to the stability of the HEWL-antibody scFv-10 complex. *Biochemistry* submited.

Rajpal A, Taylor MG, Kirsch JF. 1998. Quantitative evaluation of the chicken lysozyme epitope in the HyHEL-10 Fab complex: free energies and kinetics. *Protein Sci 7* : 1868-1874

Schreiber G, Fersht AR. 1995. Energetics of protein-protein interactions: analysis of the barnase-barstar interface by single mutations and double mutant cycles. *J Mol Biol 248* : 478-486.

Schreiber G, Frisch C, Fersht AR. 1997. The role of Glu73 of barnase in catalysis and binding of barstar. *J Mol Biol 270* : 111-122.

Serrano L, Horovitz A, Avron B, Bycroft M, Fersht AR. 1990. Estimating the contribution of engineered surface electrostatic interactions to protein stability by using double-mutant cycles. *Biochemistry 29* : 9343-9352.

Serrano L, Kellis JTJ, Cann P, Matouschek A, Fersht AR. 1992. The folding of an enzyme- II. substructure of barnase and the contribution of different interactions to protein stability. *J Mol Biol 224* : 783-804.

Smith-Gill SJ, Lavoie TB, Mainhart CR. 1984. Antigenic regions defined by monoclonal antibodies correspond to structural domains of avian lysozyme. *J Immunol 133* : 384-392.

Souza SC, Frick GP, Wang X, Kopchick JJ, Lobo RB, Goodman HM. 1995. A single arginine residue determines species specificity of the human growth hormone receptor. *Proc Natl Acad Sci USA 92* : 959-963.

Taylor MG, Rajpal A, Kirsch JF. 1998. Kinetic epitope mapping of the chicken lysozyme/HyHEL-10 Fab complex: delineation of docking trajectories. *Protein Sci* 7 : 1857-1867

Tsumoto K, Ogasahara K, Ueda Y, Watanabe K, Yutani K, Kumagai I. 1995. Role of Tyr residues in the contact region of anti-lysozyme monoclonal antibody HyHEL-10 for antigen binding. *J Biol Chem 270* : 18551-18557.

Tsumoto K, Ogasahara K, Ueda Y, Watanabe K, Yutani K, Kumagai I. 1996. Role of salt Bridge formation in antigen-antibody Interaction. *J Mol Biol 271* : 32612-32616.

Wells JA. 1996. Binding in the growth hormone receptor complex. *Proc Natl Acad Sci USA 93* : 1-6.

Xavier KA, Willson RC. 1998. Association and dissociation kinetics of anti-hen egg lysozyme monoclonal antibodies HyHEL-5 and HyHEL-10. *Biophys J 74* : 2036-2045.

Ysern X, Li H, Mariuzza RA. 1998. Imperfect interfaces [news]. *Nature Struct Biol 5* : 412-414.

Table 1. *Crystallographically identified contacts in the HyHEL-10/Lysozyme (HEWL) interface* [a]

HyHEL-10	HEWL	HyHEL-10	HEWL
V_L		V_H	
G30	G16	T30[c]	R73(h)
N31	H15, G16, **K96**(h)[b]	S31	R73(h), L75
N32	G16(h), **Y20**	D32	**K97**(s)
Y50	N93, **K96**	Y33	W63, **K97**(h), I98, S100, D101
Q53	T89, N93(h)	Y50	R21(h), S100(h)
S91	**Y20** (h)	S52	D101
N92	**Y20**, R21(h)	Y53	W63, L75, D101(h)
Y96	R21 (h)	S54	D101
		S56	D101, G102
		Y58	R21, S100, G102(h)
		W95	R21, **K97**, S100

[a] Padlan *et al.*, 1989.

[b] Codes: h: hydrogen bond (See Table 2 for donor/acceptor identification.); s: salt bridge.

The HEWL residues highlighted in bold have been identified as major contributors to the free energy of complex formation by alanine scanning mutagenesis (Rajpal *et al.*, 1998). The contributions of the underlined HyHEL-10 side chain residues were evaluated in this work.

[c] Framework residue

Table 2. *Double mutant cycle analysis of the coupling energies between the indicated mutant pairs in the HyHEL-10/HEWL complex for adjacent partners* [a]

HyHEL-10 mutants	$\Delta\Delta G^b$ (kcal/mol) HyHEL-10 mutants	HEWL mutants	$\Delta\Delta G^b$ (kcal/mol) HEWL mutants	Double mutant $\Delta\Delta G^b$ (kcal/mol)	Lost Interaction[a]	$\Delta\Delta G_{int}{}^c$ (kcal/mol)
V_L						
$N31_LA$	5.2 ± 0.1	K96A	7.0 ± 0.3	7.5 ± 0.3	H bond	4.7 ± 0.4
$Y50_LA$	4.6 ± 0.1	K96A	7.0 ± 0.3	7.8 ± 1.0	v der W	3.8 ±1.1
$Y96_LA$	2.7 ± 0.1	R21A	1.1 ± 0.1	5.7 ± 0.3	H bond	-1.9 ± 0.3
V_H						
$D32_HA$	1.9 ± 0.1	K97A	6.2 ± 0.1	4.6 ± 0.2	Salt bridge	3.5 ± 0.2
$Y33_HA$	6.0 ± 0.1	K97A	6.2 ± 0.1	7.2 ± 0.2	v der W+ main chain H bond	5.0 ± 0.2
$Y50_HA$	7.4 ± 0.4	R21A	1.1 ± 0.1	8.0 ± 0.7	H bond	0.5 ± 0.8
$W95_HA$	5.5 ± 0.2	K97A	6.2 ± 0.1	NB[d]	v der W	NA[e]

[a] Structural data from Padlan *et al* , 1989

[b] The $\Delta\Delta G$ values are defined as $\Delta\Delta G = RT \ln \frac{K_{mut\_complex}}{K_{WT\_complex}}$; where K is the dissociation constant.

[c] Coupling energies are defined as $\Delta\Delta G_{int} = \Delta\Delta G_{A\text{-}A'}$ (column 2) + $\Delta\Delta G_{B\text{-}B'}$(column 4) – $\Delta\Delta G_{AB\text{-}A'B'}$(column 5); A and B refer to residues present in WT HyHEL-10 and HEWL

respectively, A' and B' represent residues present in mutant HyHEL-10 and HEWL respectively.

[d] NB, no binding at 20 μM HyHEL-10: K_D> 40μM, ΔΔG > 8.5 kcal/mol.

[e] Not available, see (d)

Table 3. *Donor/acceptor double mutagenesis evaluations of the free energy contributions of the hydrogen bonds in the HyHEL-10/HEWL complex*

HyHEL10	HEWL	$\Delta\Delta G^a$ kcal/mol (scFv-10 mutation)	$\Delta\Delta G^b$ kcal/mol (HEWL mutation)
V_L			
N31 Oδ1	K96 Nζ	5.2 ± 0.1 ($N31_LA$)	6.8 ± 0.1 (K96M)
N32 Nδ2	G16 O	5.1 ± 0.1 ($N32_LA$)	
Q53 Oε1 Q53 Nε2	N93 Nδ2 N93 Oδ1	1.0 ± 0.2 ($Q53_LA$)	0.6 ± 0.1 (N93A)
S91 O	Y20 OH		-0.4 ± 0.1 (Y20F)
Y96 OH	R21 NH1	1.4 ± 0.2 ($Y96_LF$)	1.1 ± 0.1 (R21A)
V_H			
S31 Oγ	R73 NH1	0.2 ± 0.3 ($S31_HA$)	-0.3 ± 0.1 (R73A)
T30 O	R73 NH1		-0.3 ± 0.1 (R73A)
Y33 OH	K97 O	1.1 ($Y33_HF$)[c]	
Y50 OH	R21 NH1, S100 O	1.7 ($Y50_HF$)[c]	1.1 ± 0.1 (R21A)
Y53 O	D101 Oδ1		1.5 ± 0.1 (D101A)
Y58 OH	G102 N	0.4 ($Y58_HF$)[c]	

a $\Delta\Delta G = RTln(K_d[\text{mutant scFv-10 complex}]/K_d[\text{WT scFv-10 complex}])$ with wt HEWL.

b $\Delta\Delta G = RTln(K_d[\text{mutant HEWL complex}]/K_d[\text{WT HEWL complex}])$ with wt scFV-10.

c Values from Tsumoto *et al* ., (1995)

Table 4. *Double mutant cycle analysis of the coupling energies between the indicated mutant pairs in the HyHEL-10-HEWL complex for non-contacting residues*

HyHEL-10 mutants	$\Delta\Delta G^b$ (kcal/mol) HyHEL-10 mutants	HEWL mutants	$\Delta\Delta G^b$ (kcal/mol) HEWL mutants	$\Delta\Delta G^b$ (kcal/mol) Double mutant	Distance between residues[c] (Å)	$\Delta\Delta G_{int}$[d] (kcal/mol)
V_L						
$Y50_LA$	4.6 ± 0.1	Y20A	4.9 ± 0.1	NB[e]	5.6	NA[f]
$Y50_LA$	4.6 ± 0.1	R21A	1.1 ± 0.1	6.4 ± 0.2	9.5	-0.7 ± 0.2
$Y50_LA$	4.6 ± 0.1	K97A	6.2 ± 0.1	7.3 ± 0.6	5.8	3.5 ± 0.6
$Y50_LF$	2.4 ± 0.2	Y20A	4.9 ± 0.1	6.3 ± 0.1	5.6	1.0 ± 0.2
$Y50_LF$	2.4 ± 0.2	R21A	1.1 ± 0.1	4.4 ± 0.2	9.5	-0.9 ± 0.3
$Y50_LF$	2.4 ± 0.2	K97A	6.2 ± 0.1	NB	5.8	NA
V_H						
$W95_HA$	5.5 ± 0.2	Y20A	4.9 ± 0.1	NB	4.5	NA
$W95_HA$	5.5 ± 0.2	K96A	7.0 ± 0.3	7.7 ± 0.7	6.4	4.8 ± 0.8
$W95_HF$	3.2 ± 0.2	K96A	7.0 ± 0.3	NB	6.4	NA

[a] From Padlan *et al*, (1989).

[b] The $\Delta\Delta G$ values are defined as $\Delta\Delta G = RT \ln \frac{K_{mut\_complex}}{K_{WT\_complex}}$; where K is the dissociation constant.

[c] Closest distance between side chains for the WT residues in Å (PDB file 3HFM).

[d] Coupling energies are defined in Table 2.

[e] NB, no binding was detected at 20 μM HyHEL-10; therefore $K_D > 40\mu M$, $\Delta\Delta G > 8.5$ kcal/mol.

[f] Not available, see (e).

Table 5. *Sensitivity of propagated error in free energy of interaction calculated from double mutant cycles to the error in the individual equilibrium constants (K_D or K_A)*

σ (K_D) or σ (K_A)[a] %	σ (ΔG_A[b]) kcal/mol	σ ($\Delta\Delta G_{A\rightarrow A'}$[c]) kcal/mol	σ ($\Delta\Delta G_{int}$[d]) kcal/mol
10	0.14	0.19	0.33
20	0.27	0.38	0.67
30	0.41	0.58	1.00
50	0.68	0.96	1.67
100	1.36	1.92	3.33

[a] *Per cent* errors in the individual determination of K_D values.

[b] $RT(\sigma(K_D)/K_D)$.

[c] Propagated error for ΔG_A-$\Delta G_{A'}$.

[d] Equation 3.

Fig. 1. Left: CPK representation of HyHEL-10 paratope residues in contact with HEWL (top); and of the complementary HEWL epitope residues (bottom). Amino acids whose mutation to alanine gives a $\Delta\Delta G > 4$ kcal/mol (hot spots) are shown in red, those yielding 1 kcal/mol $<\Delta\Delta G< 4$ kcal/mol (warm spots) are in yellow and, those with < 1 kcal/mol are in blue (null spots). Correct apposition of the structures can be visualized by folding the page horizontally. To aid in the positioning, the three major immunodeterminants of HEWL (Rajpal *et al.*, 1998) are superimposed in black ball and stick models on the paratope structure (top).

Right: Histograms reporting the specific destabilization free energies for the mutations shown on the left: Upper, paratope mutants. The total bar height reflects the Tyr→Ala mutations while the values in blue show the uniformly smaller effects of Tyr→Phe mutations in the paratope (HyHEL-10). Lower: destabilization of the HyHEL-10/HEWL complex by alanine scanning mutagenesis of the epitope. The values obtained here with the scFv of HyHEL-10/HEWL complexes are within ± 0.5 kcal/mol of those previously reported for the corresponding Fab-10/HEWL complexes (Rajpal *et al.*, 1998). Literature values for the $Y53_H$ (A,F) $Y58_H$(A,F), $Y33_HF$ and $Y50_HF$ /HEWL (WT) complexes (*) are shown (Tsumoto *et al*, 1995).

Fig. 2. Correspondence between $\Delta\Delta G$ values obtained by mutation of either H-bonding partner in the HyHEL-10/HEWL. The specific mutants are labeled. The slope of the line excluding the $N31_LA$/K96M pair is 1.0.

Fig. 3. Free energy changes in the HyHEL-10/HEWL complex stability for Tyr→Phe mutation plotted against the corresponding Tyr→Ala free energy changes. The dotted line is for the residues of the light chain (slope 0.5), and the solid line is for those of the heavy chain (slope 0.2).

Scheme 1. Conservative (upper) and alanine (lower) replacement double mutant cycle analysis of the putative HyHEL-10 ($Asp32_H$) - HEWL (Lys97) salt bridge. Left: replacements of HyHEL-10 ($Asp32_H$) to Asn (upper) and Ala (lower); Right: replacements of HEWL (Lys97) by Met (upper) and Ala (lower). The numerical values are in kcal/mol and give the

$\Delta\Delta G$ with respect to the WT complex (shown at the center of the figure) that are obtained for the indicated mutations. Local charges are shown as (–) negative, (+) positive, and (O) neutral next to each complex.

Scheme 2. Dissection of the free energy contribution of the $N31_L$ -K96 hydrogen bond to the stability of the HyHEL-10/HEWL complex. Upper: Replacement of the neutral/positive hydrogen bond with a putative salt bridge by $N31_LD$ and $N31_LE$ mutations. Lower: Alanine replacement double mutant cycle. The numerical values are in kcal/mol and give the $\Delta\Delta G$ with respect to the WT complex (shown at the center of the figure) that are obtained for the indicated mutations. Local charges are shown as (–) negative, (+) positive, and (O) neutral next to each complex.

Appendix. *Experimental data set*

Complex (scFV-*HEL*)	k_{on} (10^6 M^{-1} s^{-1})	err k_{on} (10^6 M^{-1} s^{-1})	k_{off} (10^{-4} 1/s)	err k_{off} (10^{-4} 1/s)	K_D (nM)	err K_D (nM)	$\Delta\Delta G$ (kcal/mol)	err $\Delta\Delta G$ (kcal/mol)
wt-*wt*	1.88	0.08	0.54	0.002	0.03	0.001	-	-
Interaction HEL Y20								
wt-*Y20A*					113	8	4.9	0.11
N32LA-*wt*					167	27	5.13	0.22
N32LA-*Y20A*					NO binding at 4 µM scFv			
Interaction HEL K96								
wt-*K96A*					4000	800	7.00	0.27
N31LA-*wt*					200	20	5.20	0.15
N31LA-*K96A*					9000	2000	7.5	0.30
N31LD-*wt*	1.26	0.07	3.68	0.7	0.29	0.06	1.4	0.28
N31LE-*wt*					460	40	5.7	0.13
Y50LA-*wt*					66	6	4.6	0.13
Y50LL-*wt*					50	4	4.4	0.12
Y50LF-*wt*	1.25	0.02	20.6	2.5	1.6	0.2	2.4	0.18
Y50LA-*R21A*					1400	200	6.4	0.19
Y50LF-*R21A*					45	6	4.36	0.19
Y50LF-*Y20A*					1100	100	6.3	0.13
Y50LA-*K96A*					14000	11000	7.8	1.06
Y50LA-*K97A*					7000	3000	7.30	0.58
Y50LF-*K97A*					NO binding at 20 µM scFv			
Y50LF-*K96A*					NO binding at 20 µM scFv			
Y50LA-*Y20A*					NO binding at 8 µM scFv			
Interaction HEL K97								

wt-*K97A*					1000	50	6.2	0.08
Y33$_H$A-*wt*					800	80	6.0	0.15
Y33$_H$A-*K97A*					6000	1000	7.2	0.23
Y33$_H$A-*K96A*					NO binding at 10 μM scFv			
Y33$_H$A-*Y20A*					NO binding at 10 μM scFv			
[a]Y33$_H$F-*wt*							1.1	
W95$_H$F-*K97A*					NO binding at 20 μM scFv			
W95$_H$F-*wt*					7.2	0.8	3.27	0.16
W95$_H$F-*Y20A*					1110	80	6.26	0.11
W95$_H$A-*wt*					330	40	5.5	0.17
W95$_H$A-*K97A*					No binding at 10 μM scFv			
W95$_H$A-*K96A*					14000	7000	7.7	0.68
W95$_H$F-*K96A*					No binding at 10 μM scFv			
W95$_H$A-*Y20A*					LOW binding at 8 μM scFv			
D32$_H$A-*wt*	1.6	0.1	11.90	0.1	0.74	0.03	1.93	0.07
D32$_H$A-*K97A*					70	10	4.62	0.19
D32$_H$N-*K97A*					116	7	4.92	0.09
D32$_H$N-*wt*	2.01	0.04	0.33	0.1	0.04	0.01	0.2	0.3
D32$_H$A-*K97M*	2.9	0.1	5.8	0.3	0.2	0.01	1.14	0.08
D32$_H$N-*K97M*	2.46	0.1	1.12	0.01	0.05	0.002	0.27	0.07
wt-*K97M*	1.53	0.05	2.8	0.1	0.19	0.01	1.1	0.08
Non Interacting with HEL Hot Spots								
wt-*R21A*	1.56	0.06	2.71	0.16	0.17	0.01	1.07	0.09
S31$_H$A-*wt*	1.24	0.06	0.48	0.08	0.04	0.01	0.18	0.34
Y50$_H$A-*wt*					7000	2000	7.4	0.39
[a]Y50$_H$F-*wt*							1.7	

Y50HA-*R21A*					20000	10000	8.0	0.68
Q53LA-*wt*	1.37	0.05	2.0	0.2	0.15	0.02	0.96	0.18
Y96LA-*wt*	0.8	0.03	23.00	0.06	2.9	0.11	2.73	0.07
Y96LA-*R21A*					500	100	5.7	0.27
Y96LF-*R21A*					35	5	4.21	0.19
Y96LF-*wt*	1.4	0.1	4.5	0.3	0.32	0.04	1.43	0.18
[a]**Y53HA**-*wt*							3.3	
[a]**Y53HF**-*wt*							0.7	
[a]**Y58HA**-*wt*							1.7	
[a]**Y58HF**-*wt*							0.4	

[a]From Tsumoto *et al* , 1995.

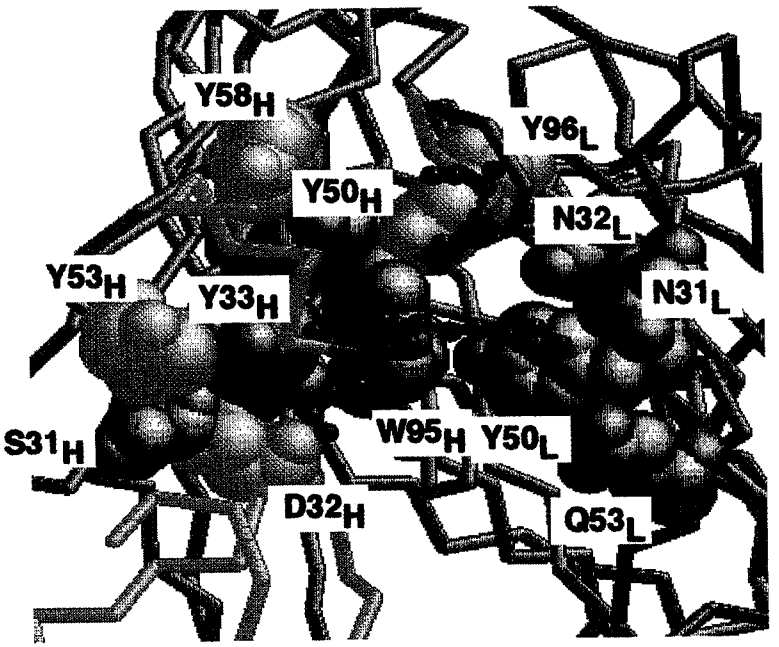
Y58H
Y96L
Y50H
N32L
Y53H
Y33H
N31L
S31H
W95H
Y50L
D32H
Q53L

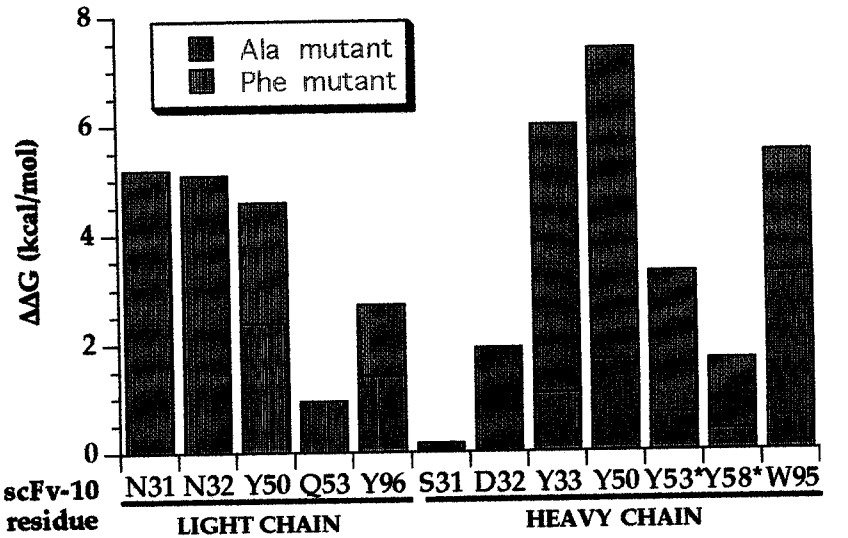
Ala mutant
Phe mutant
ΔΔG (kcal/mol)
0
2
4
6
8
scFv-10 residue
N31 N32 Y50 Q53 Y96 S31 D32 Y33 Y50 Y53* Y58* W95
LIGHT CHAIN
HEAVY CHAIN

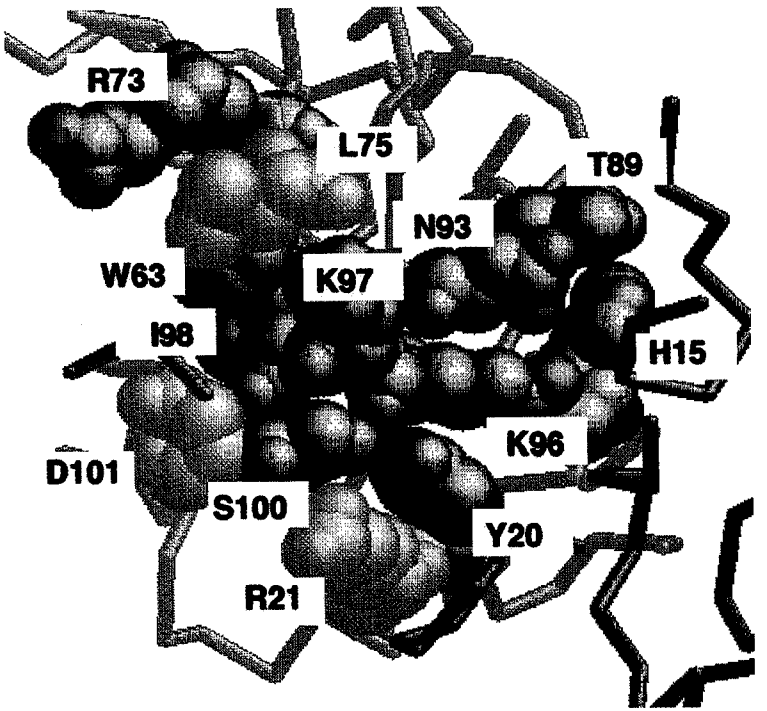
R73
L75
T89
N93
W63
K97
I98
H15
K96
D101
S100
Y20
R21

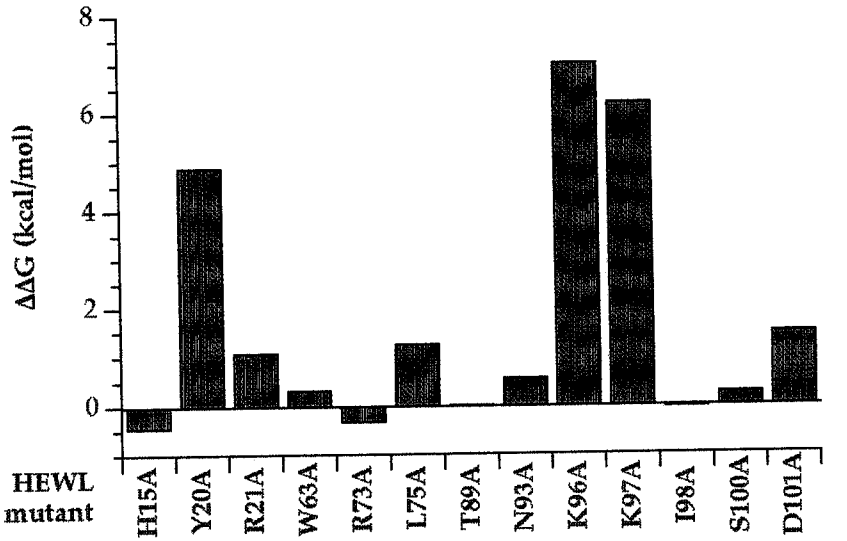
ΔΔG (kcal/mol)
0
2
4
6
8
HEWL mutant
H15A
Y20A
R21A
W63A
R73A
L75A
T89A
N93A
K96A
K97A
I98A
S100A
D101A

Fig 2

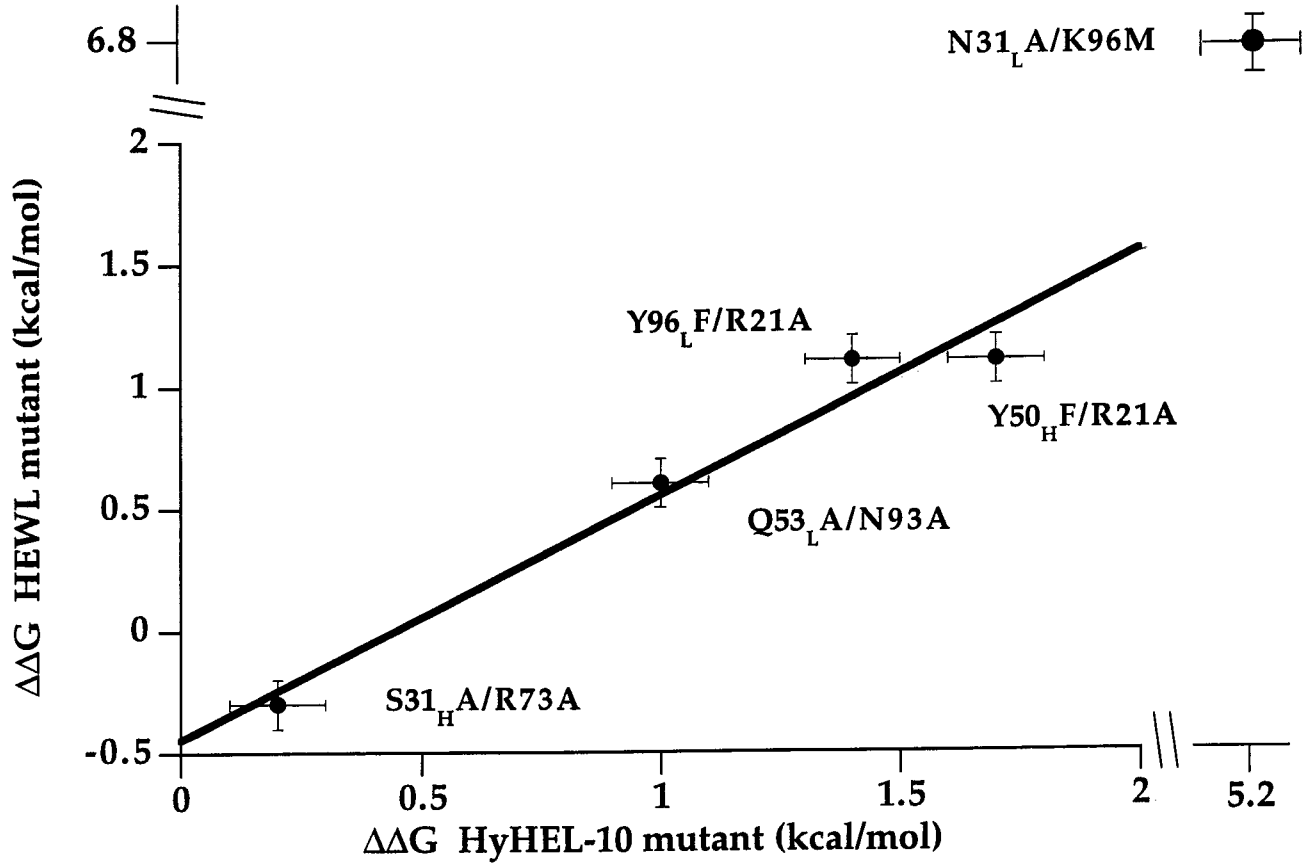
6.8
N31$_L$A/K96M
2
1.5
1
0.5
0
-0.5
Y96$_L$F/R21A
Y50$_H$F/R21A
Q53$_L$A/N93A
S31$_H$A/R73A
0
0.5
1
1.5
2
5.2
ΔΔG HEWL mutant (kcal/mol)
ΔΔG HyHEL-10 mutant (kcal/mol)

Fig 3

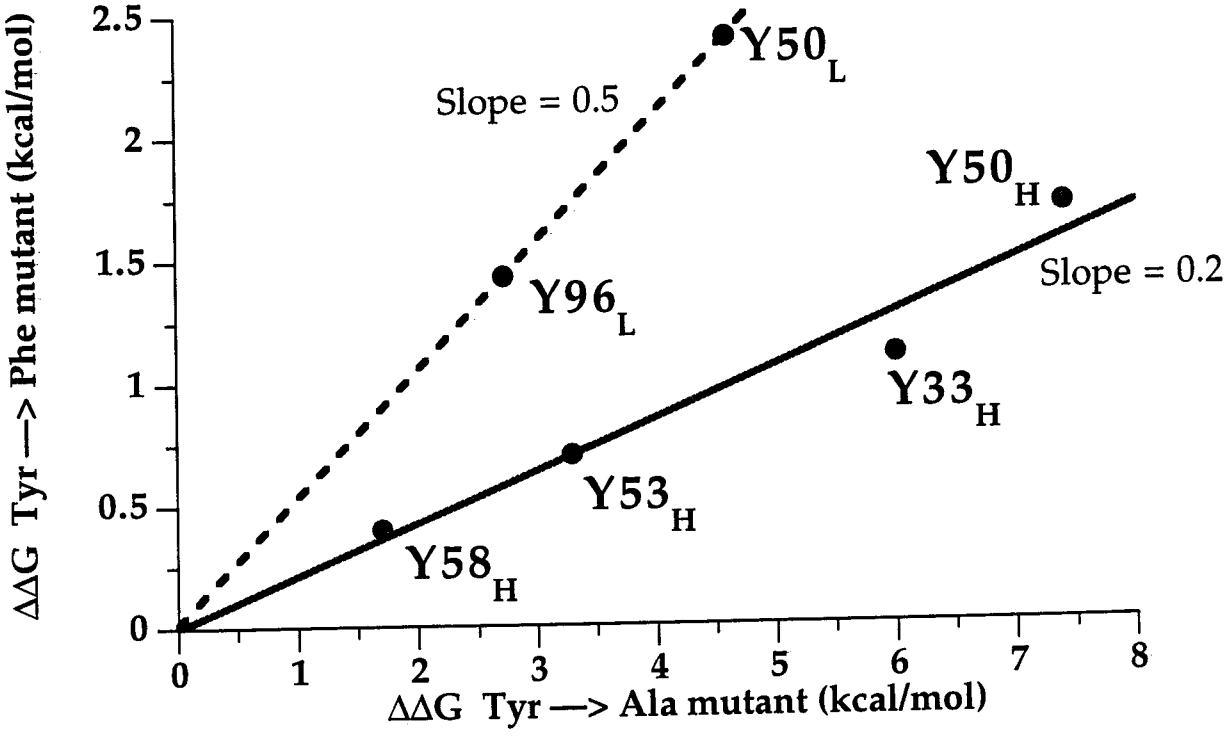
2.5
2
1.5
1
0.5
0
0
1
2
3
4
5
6
7
8
ΔΔG Tyr —> Phe mutant (kcal/mol)
ΔΔG Tyr —> Ala mutant (kcal/mol)
Slope = 0.5
Slope = 0.2
Y50L
Y50H
Y96L
Y33H
Y53H
Y58H

Scheme 1

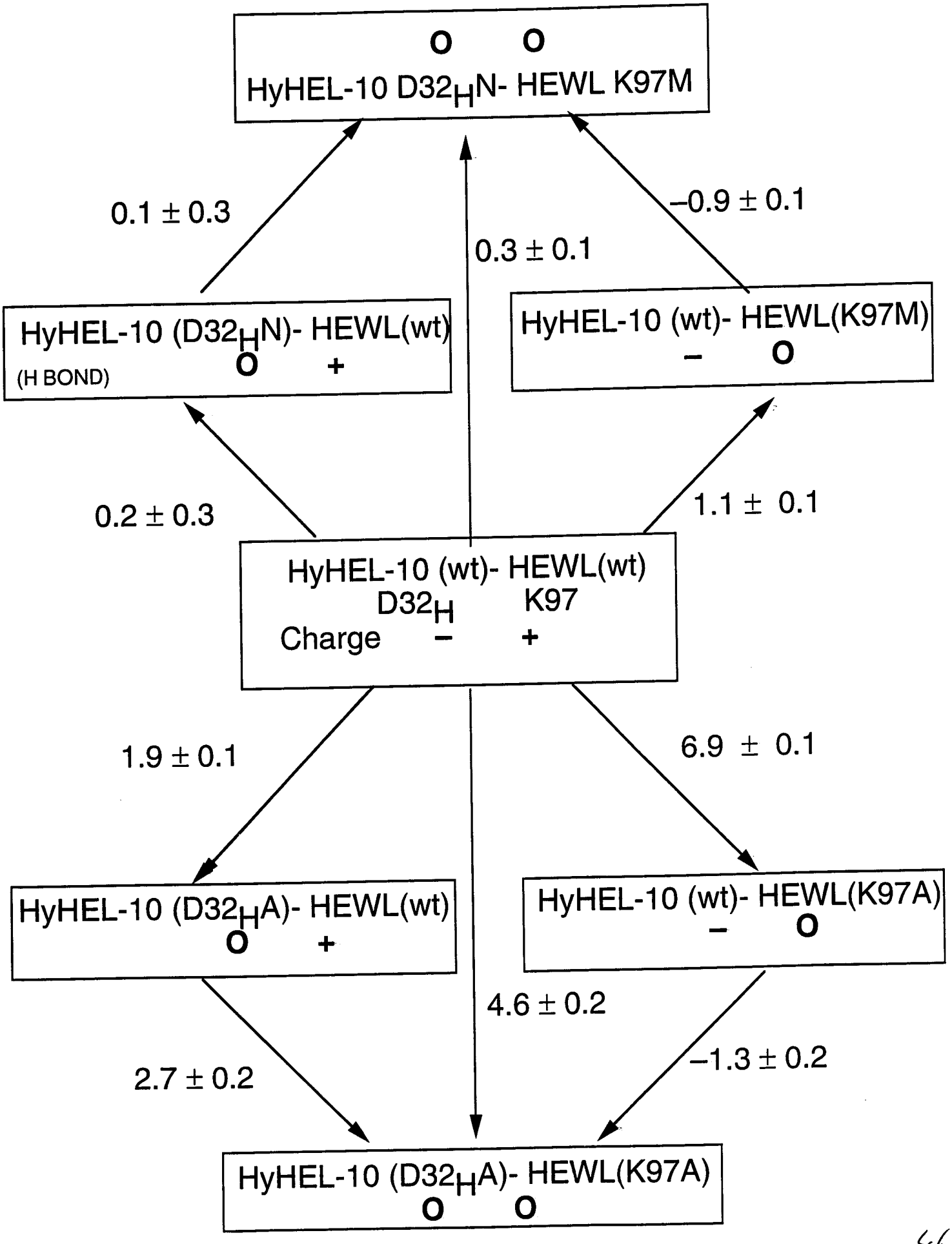
O O
HyHEL-10 D32$_H$N- HEWL K97M
0.1 ± 0.3
0.3 ± 0.1
–0.9 ± 0.1
HyHEL-10 (D32$_H$N)- HEWL(wt)
(H BOND)
O +
HyHEL-10 (wt)- HEWL(K97M)
– O
0.2 ± 0.3
1.1 ± 0.1
HyHEL-10 (wt)- HEWL(wt)
D32$_H$ K97
Charge – +
1.9 ± 0.1
6.9 ± 0.1
HyHEL-10 (D32$_H$A)- HEWL(wt)
O +
HyHEL-10 (wt)- HEWL(K97A)
– O
4.6 ± 0.2
2.7 ± 0.2
–1.3 ± 0.2
HyHEL-10 (D32$_H$A)- HEWL(K97A)
O O

Scheme 2

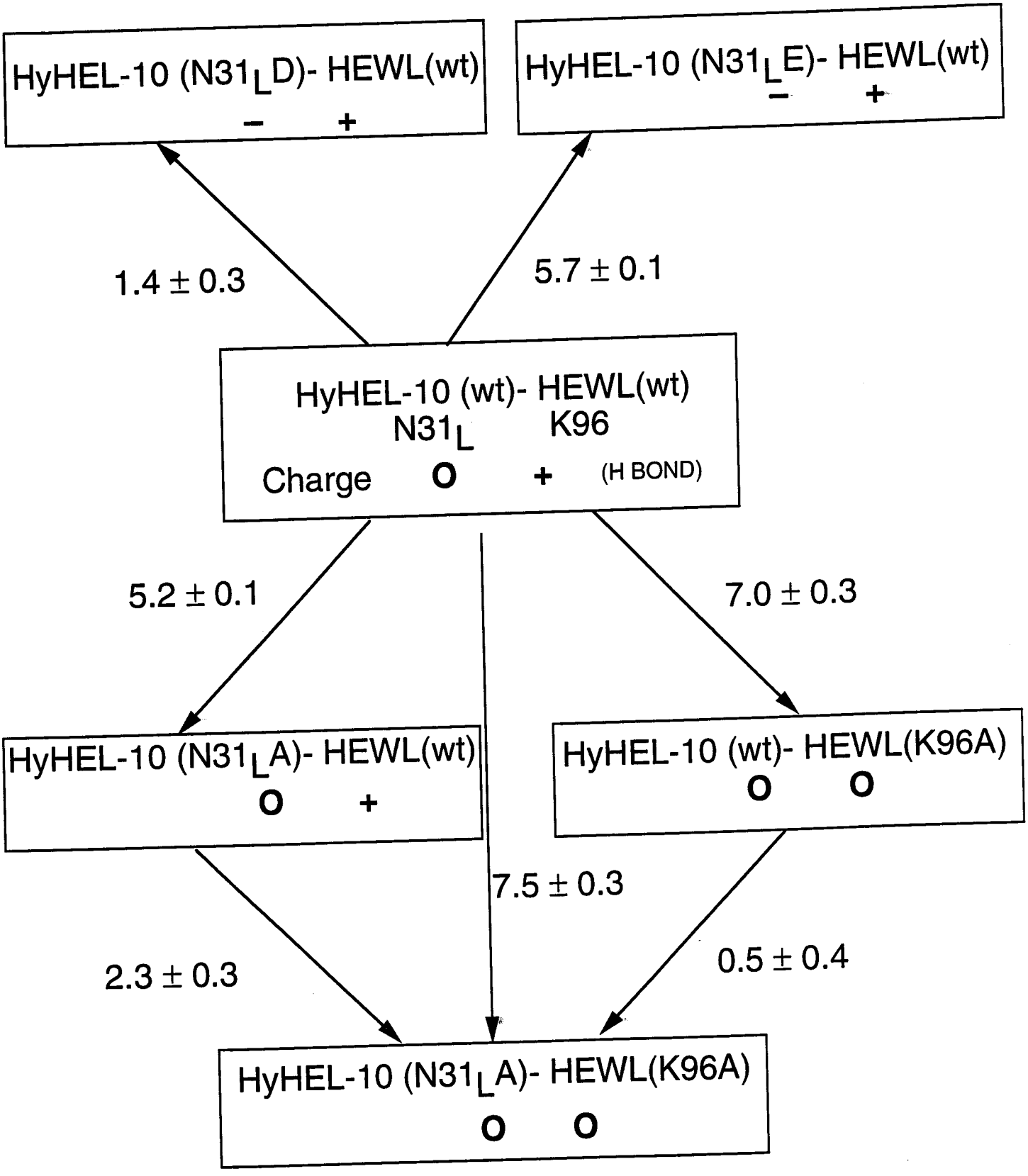
HyHEL-10 (N31$_L$D)- HEWL(wt)
– +
HyHEL-10 (N31$_L$E)- HEWL(wt)
– +
1.4 ± 0.3
5.7 ± 0.1
HyHEL-10 (wt)- HEWL(wt)
N31$_L$ K96
Charge O + (H BOND)
5.2 ± 0.1
7.0 ± 0.3
HyHEL-10 (N31$_L$A)- HEWL(wt)
O +
HyHEL-10 (wt)- HEWL(K96A)
O O
7.5 ± 0.3
2.3 ± 0.3
0.5 ± 0.4
HyHEL-10 (N31$_L$A)- HEWL(K96A)
O O